The Journal of Chemical Physics

Ab initio potential energy surfaces and nonadiabatic couplings involved in $Be^{4+}+H_2$ electron rearrangement

Cite as: J. Chem. Phys. **106**, 172 (1997); https://doi.org/10.1063/1.473033
Submitted: 30 April 1996 . Accepted: 24 September 1996 . Published Online: 31 August 1998

L. F. Errea, J. D. Gorfinkiel, E. S. Kryachko, A. Macías, L. Méndez, and A. Riera

View Online Export Citation

ARTICLES YOU MAY BE INTERESTED IN

Perspective: Nonadiabatic dynamics theory
The Journal of Chemical Physics **137**, 22A301 (2012); https://doi.org/10.1063/1.4757762

Interpolation of diabatic potential-energy surfaces: Quantum dynamics on ab initio surfaces
The Journal of Chemical Physics **123**, 134110 (2005); https://doi.org/10.1063/1.2047569

Accurate first-derivative nonadiabatic couplings for the H_3 system
The Journal of Chemical Physics **115**, 4640 (2001); https://doi.org/10.1063/1.1390510

Lock-in Amplifiers up to 600 MHz
Watch

AIP Publishing

© 1997 American Institute of Physics.

Ab initio potential energy surfaces and nonadiabatic couplings involved in $Be^{4+}+H_2$ electron rearrangement

L. F. Errea and J. D. Gorfinkiel
Departamento de Química, C-IX, Universidad Autónoma de Madrid, Cantoblanco, E-28049 Madrid, Spain

E. S. Kryachko[a] and A. Macías
Instituto de Estructura de la Materia, CSIC, Serrano 119-123, E-28006 Madrid, Spain

L. Méndez and A. Riera
Departamento de Química, C-IX, Universidad Autónoma de Madrid, Cantoblanco, E-28049 Madrid, Spain

(Received 30 April 1996; accepted 24 September 1996)

We present the main characteristics of the energy and coupling surfaces for the BeH_2^{4+} quasimolecule, that are relevant to the dynamics of electron capture in $Be^{4+}+H_2$ collisions in the 50 eV amu$^{-1}<E<1$ keV amu^{-1} energy range. To construct the wave functions, we implemented a block-diagonalization method using the many electron description standard (MELD) program, which was recently modified to calculate nonadiabatic couplings. © *1997 American Institute of Physics.* [S0021-9606(97)00301-2]

I. INTRODUCTION

The main characteristics of the potential energy curves and nonadiabatic couplings for XH^{q+} quasimolecules, as well as their relevance to the dynamics of electron capture in collisions between multicharged ions and H atoms are very well known.[1–3] On the other hand, the information on the corresponding triatomic systems XH_2^{q+} is scanty, which is unfortunate because $X^{q+}+H_2$ collisions are just as important, from the point of view of ion-beam scattering experiments as well as in the physics of thermonuclear reactors. In particular, dynamics involving Be ions is of great importance in the modeling of tokamak plasmas, because beryllium is currently used (JET) and envisaged (ITER) as a cladding for facing components (e.g., divertors), as well as a neutron multiplier in the tritium breeding blanket of fusion reactors.[4] The role of collisions between ionized Be and H_2 molecules in the ground as well as excited vibrational states is believed to play a crucial role in divertor physics. To assess its quantitative relevance, it is required to insert the corresponding capture cross sections in the modeling codes for the plasma dynamics. As a first step towards obtaining these data, in a recent paper[5] we reported some preliminary calculations on the charge transfer cross section in $Be^{4+}+H_2(X\ ^1\Sigma_g^+, v=0)$ collisions at impact energies 50 eV amu$^{-1}<E<1$ keV amu^{-1}). This dynamical treatment employed molecular energies and nonadiabatic couplings for the BeH_2^{4+} quasimolecule calculated with the multireference configuration interaction (CI) program MELD,[6] which was recently modified[7] to obtain the couplings. Here, we shall report the characteristics of the molecular data, which for conciseness could not be presented in our dynamical work,[5] and are a useful quantitative reference for future applications on electron rearrangement occurring at pseudocrossings, in multicharged ion–H_2 collisions.

Application of the techniques of *ab initio* quantum chemistry in the treatment of dynamical, nonreactive problems would seem straightforward, since spectroscopic accuracy in the electronic data is not usually required. However, one finds that several standard techniques, and many usual characteristics of potential energy surfaces (PES's), do not directly apply. For instance, unlike the ''usual'' situation, the electronic states of the triatomic involved in nonreactive collisions are seldom bound (no ''equilibrium'' geometry), and nonadiabatic couplings are also needed. For descriptions and references of state-of-the-art techniques of quantum chemistry to calculate PES's, see, for example, Searles and Nagy-Felsobuki[8] for molecular vibrorotational spectra, and Handy *et al.*[9] for reaction dynamics; for dynamical couplings, see, e.g., Nakamura.[10]

The BeH_2^{4+} quasimolecule is a striking case where the usual techniques of quantum chemistry need modification in a way that will not be found in those publications. As will be explained in the next section, this is due to the fact that the electronic states of both the entrance and the main exit channels are infinitely excited, because their energies lie above those of several Rydberg series. This precludes a direct application of the usual variational methods, which are based on the Hylleraas–Undheim[11]–McDonald[12] theorem: to accurately reproduce the states, an infinite basis would seem to be necessary! To solve the problem, the present work reports an implementation of the so-called block-diagonalization (BD) approach,[13–15] which is here applied to a triatomic for the first time; the method is described in Sec. II A. Once the technique is implemented, we shall show in Sec. II B that the calculation of dynamical couplings follows as in the standard CI case.[7] Section III presents and discusses the main overall features of the PES's, and the radial coupling that determines the capture process in the $Be^{4+}+H_2(X\ ^1\Sigma_g^+)$ dynamics. The variation of the molecular data with angular and radial internal coordinates will be examined in detail, as it has a strong bearing on the use of standard approximations[16–20] to calculate vibrationally resolved cross sections.

[a]Permanent address: Bogoliubov Institute for Theoretical Physics, Kiev, Ukraine 252143.

 0021-9606/97/106(1)/172/10/$10.00 © 1997 American Institute of Physics

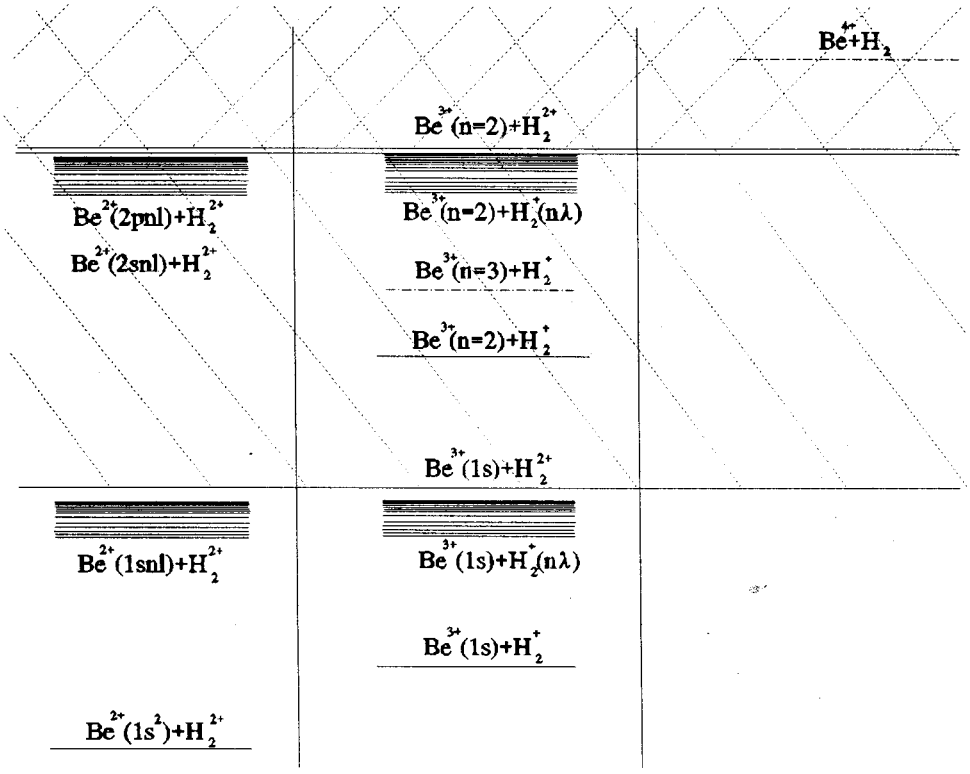

FIG. 1. Qualitative diagram illustrating the infinitely excited character of the electronic energies that are relevant to electron rearrangement in $Be^{4+}+H_2$ collisions, at infinite Be–H separations. For clarity, the molecular energies are represented by three blocks of short horizontal lines: (i) The left block corresponds to states of character $Be^{2+}+H^++H^+$, and contains the Rydberg series $Be^{2+}(1snl)+H^++H^+$ converging to the first ionization threshold $Be^{3+}(1s)+H^++H^+$ (marked with a long horizontal line), the second Rydberg series of autoionizing states $Be^{2+}(2snl)+H^++H^+$, $Be^{2+}(2pnl)+H^++H^+$ converging to the second ionization threshold, and so on. (ii) The middle bloc contains the Rydberg series $Be^{3+}(1s)+H_2^+(n\lambda)$ converging to the first ionization threshold. Above this threshold, we have autoionizing states of structure $Be^{3+}(n=2,3)+H_2^+(n\lambda)$, etc., and in particular, the relevant exit channels, of structure $Be^{3+}(3l)+H_2^+(1s\sigma)$, which are therefore seen to be infinitely excited. (iii) The right block contains the entrance channel $Be^{4+}+H_2(^1\Sigma_g^+)$ energy. This state is therefore seen to be infinitely excited.

Atomic units are used throughout, except where otherwise indicated.

II. METHOD

A. Molecular energies: BD using MELD

The BeH_2^{4+} geometry can be defined by the usual internal coordinates:[21] the two ''bond'' lengths $R\equiv R_{\mathrm{Be-H}}$, $r\equiv R_{\mathrm{H-H}}$, and the angle θ between them.

For the collision energy range 50 eV $\mathrm{amu}^{-1}<E<1$ keV amu^{-1}, the main outcome in $Be^{4+}+H_2(X\ ^1\Sigma_g^+)$ collisions is[5] single charge transfer to molecular channels Ψ_{sct}, which are correlated at infinite R separations, to $Be^{3+}(3l)+H_2^+(1s\sigma)$. These states transform like irreducible representation of the point group C_s, and are, as mentioned in Sec. I, infinitely excited. This may be seen in the qualitative diagram of Fig. 1 for the $R\rightarrow\infty$ limit.

In addition to this complication, the energies of Ψ_{ent} and Ψ_{sct} present avoided crossings with those of other infinitely excited wave functions Ψ_{dct}, of electronic structure $Be^{2+}+(2snl)+H^++H^+$, $Be^{2+}(2pnl)+H^++H^+$, which describe double capture to autoionizing Be ions. These avoided crossings are physically irrelevant, because they are very sharp, and hence diabatically traversed except at extremely low nuclear velocities. This sharpness may be understood by considering the dominant configurational structure of the Ψ_{ent}, Ψ_{sct}, and Ψ_{dct} wave functions outside the regions where their energies pseudocross. At the rather large R (>5 bohr) distances that are involved in the electron transfer dynamics, this structure is of the form

$$\begin{aligned}
\Psi_{\mathrm{ent}} &\approx \|\sigma_{\mathrm{H-H}}\overline{\sigma_{\mathrm{H-H}}}\|,\\
\Psi_{\mathrm{sct}} &\approx \frac{1}{\sqrt{2}}\left(\|\sigma'_{\mathrm{H-H}}\,\overline{\chi_{\mathrm{Be}}}\|-\|\overline{\sigma'_{\mathrm{H-H}}}\chi_{\mathrm{Be}}\|\right),\\
\Psi_{\mathrm{dct}} &\approx \frac{1}{\sqrt{2}}\left(\|\chi_{\mathrm{Be}}\overline{\chi'_{\mathrm{Be}}}\|-\|\overline{\chi_{\mathrm{Be}}}\chi'_{\mathrm{Be}}\|\right)
\end{aligned} \tag{1}$$

in a standard notation, where $\sigma_{\mathrm{H-H}}$, $\sigma'_{\mathrm{H-H}}$ are molecular orbitals (MO's) of the H_2 and H_2^+ systems, respectively, and χ_{Be}, χ'_{Be} atomic orbitals. Whenever the energies of two of these configurations cross, as functions of R, for fixed θ, r values, those of the corresponding adiabatic wave functions avoid crossing, and the energy gap at the pseudocrossing $\Delta E_{\mathrm{ent-sct}}$ ($\Delta E_{\mathrm{ent-dct}}$) is given as twice the configuration in-

teraction $\langle\Psi_{ent}|H|\Psi_{sct}\rangle$ ($\langle\Psi_{ent}|H|\Psi_{dct}\rangle$), where H is the fixed-nuclei electronic Hamiltonian. From Eq. (1) $\Delta E_{ent-sct}$ is expressed in terms of nuclear attraction and hybrid integrals, while $\Delta E_{ent-dct}$ is given in terms of exchange integrals. For $R>5$ bohr, the former interaction is considerably larger than the latter, and so is the resulting energy splitting at the corresponding pseudocrossing.

As a consequence of those characteristics, the energies of the states that are relevant to the dynamics appear as high lying roots of CI calculations, which pseudocross those of irrelevant configurations corresponding to double electron capture. This renders unwieldy both the static (of molecular energies and couplings) and dynamical (of transition probabilities) calculations. Fortunately, the problem of obtaining the static data for infinitely excited states has been thoroughly studied for atomic collisions: since those states are autoionizing, they can be constructed by using stabilization[22–24] or Feshbach[25–29] techniques; in the present case, it is simpler, and more appropriate to implement a BD method,[14,15] that permits, in addition, to eliminate the double capture transfer states (which would remain with a standard stabilization or Feshbach treatment).

The particular implementation of the BD method employed here within the MELD scheme consisted in selecting, in the CI basis, those configurations of $Be^{3+}(n\geqslant 3)+H_2^+$ and $Be^{4+}+H_2$ structure. For this purpose, we built the configurations from a set MO's obtained in a calculation carried out for BeH_2^{5+}, and excluding those MO's that correlate, at large R, to $Be^{3+}(1s,2s,2p)$. This was easily done since the excluded MO's are the lowest lying ones, and have no avoided crossings with higher ones, for the whole range of $R>5$ bohr considered. As the truncated MO basis is orthogonal to the $Be^{3+}(1s,2s,2p)$ orbitals, the CI basis constructed from it is unable to reproduce states of structure $Be^{3+}(1s,2s,2p)+H_2^+(n\lambda)$ and $Be^{2+}(1snl)+H^++H^+$. Since the Rydberg series are, to a very good accuracy, represented by these structures, they are not reproduced by the limited CI procedure. In addition, the double capture states, of structure $Be^{2+}(2snl)+H^++H^+$ and $Be^{2+}(2pnl)+H^++H^+$, are not reproduced either. The consequence is that the seeked-for entrance and exit channel wave functions are obtained from the lowest roots of the block-diagonalization procedure.

B. Dynamical couplings

In previous work,[7] the MELD[6] package was modified to evaluate directional derivatives for ion–molecule systems. This scheme can be directly applied to BD calculations such as those described in the previous section, and a summarized version of the method is presented here for completeness. As will be seen in the following (Sec. III B), we shall here focus on a derivative in the $\mathbf{R}$ direction, $M=\langle\Psi_1|\partial/\partial R|\Psi_2\rangle=\langle\Psi_1|\hat{\mathbf{R}}\cdot\nabla_R|\Psi_2\rangle$. Using standard numerical differentiation, this is evaluated, to first order in the step δ

$$M\approx\delta^{-1}\langle\Psi_1(\mathbf{R})|\Psi_2(\mathbf{R}+\delta\hat{\mathbf{R}})\rangle \tag{2}$$

in terms of the (delayed) overlap between wave functions for two close nuclear configurations, where for clarity only the parametric dependence upon $\mathbf{R}$ of the wave functions $\Psi_j(\mathbf{r}_1,s_{z_1},\mathbf{r}_2,s_{z_2};\mathbf{R})$ is made explicit, and the origin of electronic coordinates (kept constant) is chosen at the Be nucleus. The overlap is evaluated using a generalization[7] of the method proposed by Cooper.[30] As the wave functions are linear combinations of configurations constructed from a MO basis $\{\Phi_p\}$, we have

$$\langle\Psi_1(\mathbf{R})|\Psi_2(\mathbf{R}+\delta\hat{\mathbf{R}})\rangle=n^{-1}\ \mathrm{Tr}(P'_{12}S^*), \tag{3}$$

where P'_{12} is analogous to the transition density matrix P_{12} for states Ψ_1 and Ψ_2, except that Ψ_2 has now been evaluated at the shifted nuclear configuration $\mathbf{R}+\delta\hat{\mathbf{R}}$, and therefore P'_{12} is obtained from the coefficients of two CI calculations. S^* is the delayed overlap matrix in the MO basis, which is evaluated to first order in δ

$$\begin{aligned}&S^*_{pp}=\langle\Phi_p(\mathbf{R})|\Phi_p(\mathbf{R}+\delta\hat{\mathbf{R}})\rangle\approx 1,\\&S^*_{pq}=\langle\Phi_p(\mathbf{R})|\Phi_q(\mathbf{R}+\delta\hat{\mathbf{R}})\rangle.\end{aligned} \tag{4}$$

Expressing the MO's as linear combinations of a set of atomic orbitals $\{\phi_s(\mathbf{r}_\beta)\}$, where $\mathbf{r}_\beta$ represents the electronic coordinate with respect to nucleus β

$$\Phi_p(\mathbf{R})=\sum_s\ c_{ps}(\mathbf{R})\,\phi_s(\mathbf{r}_\beta) \tag{5}$$

and substituting Eq. (5) in Eq. (4), the matrix elements of S^* are expressed

$$\begin{aligned}&\langle\Phi_p(\mathbf{R})|\Phi_q(\mathbf{R}+\delta\hat{\mathbf{R}})\rangle\\&\quad\approx\delta\langle\Phi_p|\frac{\partial}{\partial R}|\Phi_q\rangle\\&\quad=\delta\sum_{st}\ c_{ps}\langle\phi_s|\phi_t\rangle\ \frac{\partial c_{qt}}{\partial R}+c_{ps}\langle\phi_s|\frac{\partial}{\partial R}|\phi_t\rangle c_{qt}\\&\quad\approx\sum_{st}\ c_{ps}(\mathbf{R})\langle\phi_s|\phi_t\rangle c_{qt}(\mathbf{R}+\delta\hat{\mathbf{R}})\\&\qquad+\delta c_{ps}(\mathbf{R})\langle\phi_s|\frac{\partial}{\partial R}|\phi_t\rangle c_{qt}(\mathbf{R}),\end{aligned} \tag{6}$$

where the partial derivatives are carried out keeping constant the remaining eight nuclear coordinates and the electronic ones. These matrix elements $\langle\phi_s|\partial/\partial R|\phi_t\rangle$ are then calculated by shifting the origin (at the Be nucleus) chosen in Eq. (8), to the nucleus β the orbital ϕ_t is centered at, by using the identity

$$\left.\frac{\partial\phi_t}{\partial R}\right]_{\mathbf{r}_j}=\left.\frac{\partial\phi_t}{\partial R}\right]_{\mathbf{r}_{j\beta}}+\sum_i\ \nabla\phi_t\cdot\left.\frac{\partial\mathbf{r}_{i\beta}}{\partial R}\right]_{\mathbf{r}_j}. \tag{7}$$

By using this equation, the last term of Eq. (6) is then related to matrix elements of the electronic gradient. The accuracy of the coupling depends on the step δ; it was checked that results did not change when δ was decreased from 10^{-4} to 10^{-5} bohr.

Finally, it may be pointed out that some additional information is contained in drawings of the surfaces $M(R,r,\theta)$

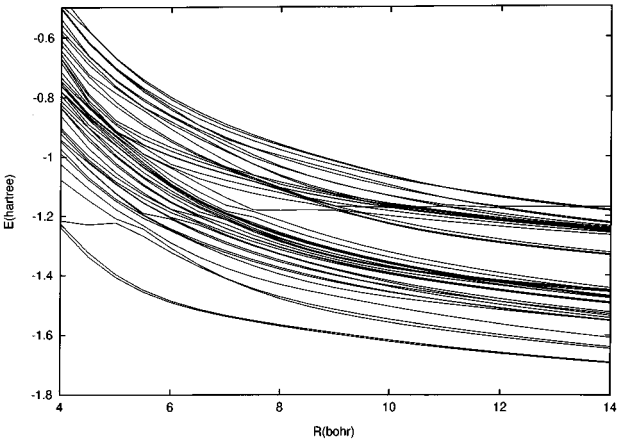

FIG. 2. Illustration of the need of the block-diagonalization procedure. Plot of the 40th to the 83rd roots (in hartree) obtained in the full-CI calculation for the BeH_2^{4+} system, by using the basis described in the text. The energies are plotted, as functions of the Be–H distance R, for a linear configuration ($\theta=0°$) and for an H–H distance $r=1.4$ bohr. This diagram may be compared to that of Fig. 3(b), using block diagonalization.

when, as in the present application: (a) the dynamical process occurs through nonadiabatic transitions between two states Ψ_1, Ψ_2 in a limited domain $R_0-\xi<R<R_0+\xi$; and (b) in this domain, the two wave functions can, to a good approximation, be represented by linear combinations of (approximately) diabatic states, which coincide with the adiabatic ones for $R<R_0-\xi$; in the present case, the diabatic states would have the structure shown in Eq. (1). Then, the surfaces $M(R,r,\theta)$ yield information on the directional derivative along the vibrational r coordinate, through

$$N(R,r,\theta)\equiv\langle\Psi_1|\partial/\partial r|\Psi_2\rangle=\langle\Psi_1|\hat{r}\cdot\nabla_r|\Psi_2\rangle \approx\int_{R_0-\xi}^{R}\frac{\partial M(R',r,\theta)}{\partial r}\,dR'. \tag{8}$$

III. RESULTS

A. BD vs CI

The orbital basis set for Be was obtained from first scaling that of Errea *et al.*,[31] and contracting it to reproduce the orbitals of $Be^{3+}(nl)$ up to $n=3$; for the H atoms we have used the 31G** basis of Krishnan *et al.*[32]

We first illustrate the difficulties involved in a straightforward application of the MELD package for the BeH_2^{4+} quasimolecule. We show in Fig. 2 a plot of the 40th to the 83rd roots obtained in a full-CI calculation, as functions of R, for fixed $\theta=0°$ and $r=1.4$ bohr. Incidentally, in view of the applications for $\theta\neq0°$ presented below, calculations were carried out disregarding any other symmetry operations that reflection on a (XZ) plane containing the nuclei. The corresponding dynamical couplings are not presented because the figure is very complicated, and is extremely difficult to obtain when one requires a sign of the couplings that is coherent for all R.

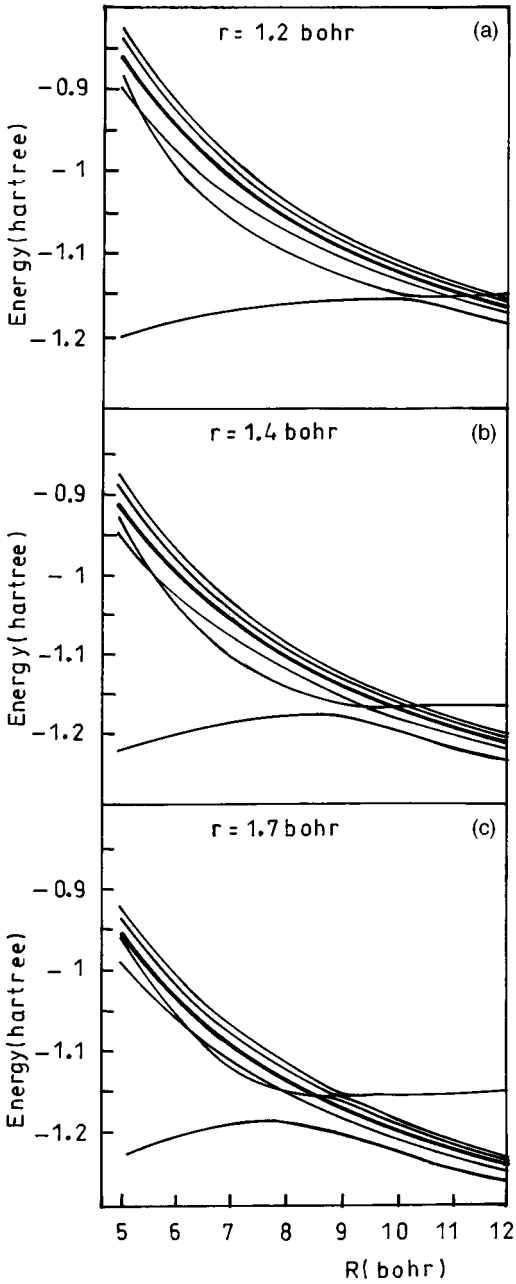

FIG. 3. Plot of the lowest roots (in hartree) obtained in the block-diagonalization calculation for the BeH_2^{4+} system. The energies are plotted, as functions of the Be–H distance R (in bohr), for a linear configuration ($\theta=0°$) and for an H–H distance (a) $r=1.2$ bohr; (b) $r=1.4$ bohr; and (c) $r=1.7$ bohr.

It is clear from Fig. 2 that elimination of the Rydberg series, discretized continuum and doubly capture states must be performed to obtain the molecular data that are needed in the dynamics. To do this, we implemented the BD method as explained in Sec. II A, thereby reducing the number of basis configurations from 551 to 370. For $\theta=0°$ and $r=1.4$ bohr, the ensuing energy correlation diagram is given in Fig. 3(b), which should be contrasted to Fig. 2. A quantitative comparison between these figures shows that, for $R>5$ bohr and except, of course, at the pseudocrossing regions, the energies

TABLE I. Illustration of the accuracy and simplification attained with the block-diagonalization procedure. Electronic energies (in a.u.) of the BeH_2^{4+} states that are relevant to electron rearrangement in $Be^{4+}+H_2$ collisions, obtained by using full configuration interaction (above) and block-diagonalization (below) methods, for three Be–H_2 distances (in a.u.). The root number is given in each case.

$\theta=0°$ R_{Be-H}	$R_{H-H}=1.4$ Channel	Root number	Energy
5.8	Entrance	52	−1.207 121
		1	−1.207 328
	Exit	69	−1.019 540
		2	−1.019 755
	Exit	70	−1.011 919
		3	−1.011 913
	Exit	72	−0.983 672
		4	−0.983 751
8.4	Entrance	69	−1.179 661
		1	−1.179 673
	Exit	70	−1.154 849
		2	−1.154 887
	Exit	73	−1.136 318
		3	−1.136 338
	Exit	75	−1.121 429
		4	−1.121 457
12.5	Exit	72	−1.243 879
		1	−1.243 887
	Exit	73	−1.233 651
		2	−1.233 655
	Exit	74	−1.226 732
		3	−1.226 738
	Entrance	84	−1.169 389
		7	−1.169 389

of the entrance and relevant exit channels are identical to the accuracy of the CI calculation. As an illustration, we give in Table I for some R values a comparison of corresponding CI and BD energies; the root numbers are also indicated. Incidentally, it will be noticed that in most cases of Table I, restriction of the basis in the BD procedure results in a (tiny) lowering of the energies. This is not contradictory to the Hylleraas–Undheim[11]–McDonald[12] theorem, and is due to the fact that the block is not strictly orthogonal to lower lying CI roots such as the $Be^{2+}(1s^2)+H_2^{2+}$ ground state. Consequently, the Hylleraas–Undheim–McDonald theorem does not apply for each isolated block. The absolute accuracy of the energies can be gauged from their asymptotic values: a comparison with other available data[33,34] for H_2 and H_2^+ is given in Table II, and the energy of $Be^{3+}(n=3)$ is reproduced to four decimal places.

TABLE II. Test of the accuracy of the asymptotic energies. Comparison between electronic energies obtained (E_{calc}) for the H_2^+ and H_2 molecules, at two H–H distances, with available accurate data (E_{exact}).

$R_{H-H}=1.4$ System	E_{calc}	E_{exact}	Ref.
H_2^+	−0.568 6	−0.569 9	33
H_2	−1.169 14	−1.174 47	34
$R_{H-H}=2.0$ System	E_{calc}	E_{exact}	Ref.
H_2^+	−0.601 59	−0.602 6	33
H_2	−1.133 45	−1.138 13	34

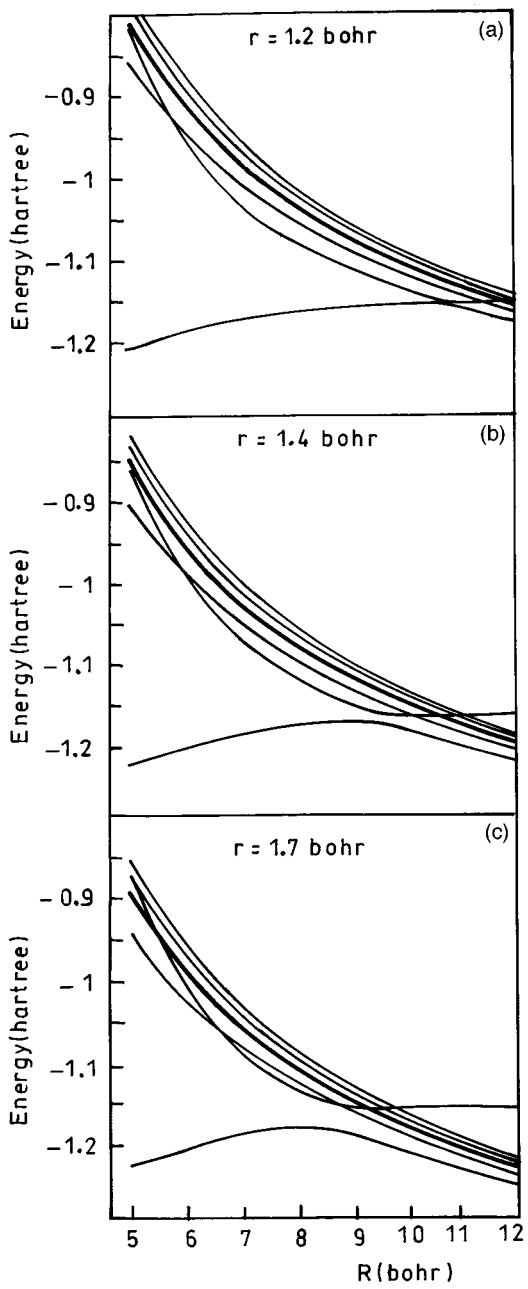

FIG. 4. Plot of the lowest roots (in hartree) obtained in the block-diagonalization calculation for the BeH_2^{4+} system. The energies are plotted, as functions of the Be–H distance R (in bohr), for a perpendicular configuration ($\theta=90°$) and for an H–H distance (a) $r=1.2$ bohr; (b) $r=1.4$ bohr; and (c) $r=1.7$ bohr.

B. Limitation to two states

A study of the molecular data permits to see which electronic states are likely to be involved in the capture process. For this, we take into account that transitions are localized[5] in the neighborhood of the pseudocrossings of the PES; see, for example, Fig. 3(b) for fixed $\theta=0°$ and $r=1.4$ bohr. Then,

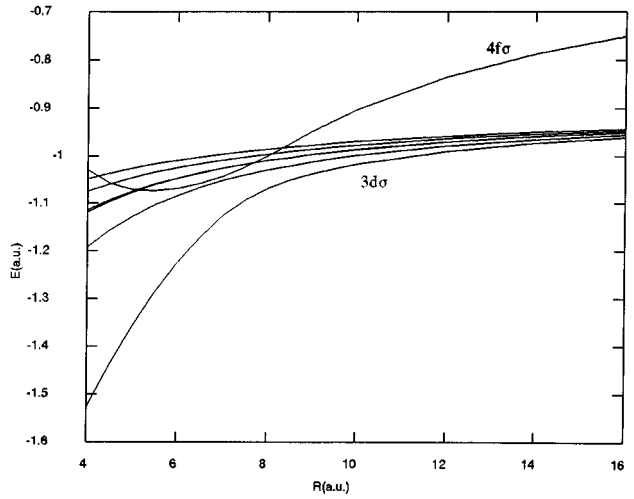

FIG. 5. Correlation plot of the (exact) molecular energies (in hartree) of the diatomic BeH^{4+} system that correlate, at infinite internuclear separation, to $Be^{4+}+H$ and $Be^{3+}(3l)+H^{+}$, and are the most relevant channels in $Be^{4+}+H$ collisions.

a straightforward study of the data displayed in this figure, together with a use of the well-known Landau–Zener model[35,36] for an order-of-magnitude estimate of the cross sections, lead to the conclusion that, at least for collisional energies $E>1$ eV and for diatomic distances $r\approx 1.4$ bohr, the dominant rearrangement mechanism involves two molecular states: the entrance channel Ψ_{ent} and a single state Ψ_{sct} correlating to $Be^{3+}(n=3)+H_2^{+}(1s\sigma)$–transitions between them taking place in the vicinity of the pseudocrossing between

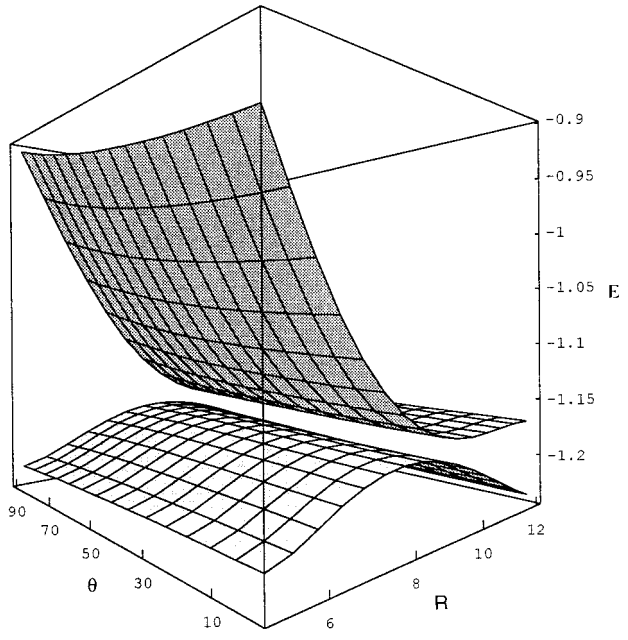

FIG. 6. Isotropy of the PES's of the entrance and main exit channel considered in this work. Plot of the electronic energies (in hartree), as functions of the Be–H distance R (in bohr), and the ''bond'' angle θ (in degrees), for an H–H distance $r=1.4$ bohr.

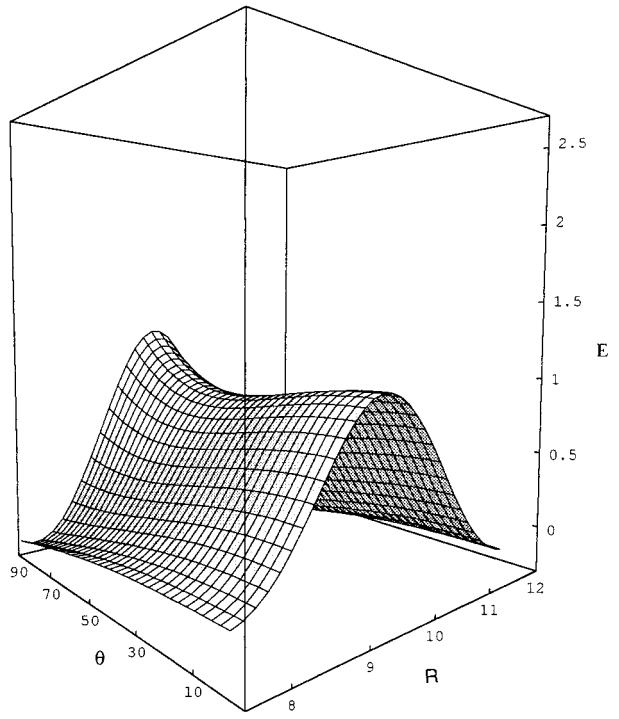

FIG. 7. Isotropy of the nonadiabatic coupling M [Eq. (2)], between the entrance and main exit channel considered in this work. Plot of M (in bohr^{-1}), as a function of the Be–H (R) (in bohr) and the ''bond'' angle θ (in degrees), for an H–H distance $r=1.4$ bohr.

their energies, located at $R\approx 9$ a.u. All other states exhibit very sharp pseudocrossings that are traversed diabatically. Similar considerations carried out for Figs. 3(a) and 3(c) show that the same diabatic character of the crossings holds for other r (1.2, 1.7 bohr, respectively) values, and in Figs. 4 for $\theta=90°$, and the same r distances. In these figures, it will be noticed that for the smallest distance $r=1.2$ bohr, the energy gaps at the sharp pseudocrossings just begin to be visible.

To understand the physical reason why only two states need to be considered, it is useful to point out the strong similarity with the energy diagram for the BeH^{4+} diatomic; this is given in Fig. 5, which can be compared to Figs. 3 for a molecular treatment of the $Be^{4+}+H(1s)\Rightarrow Be^{3+}(n=3)+H^{+}$ reaction, see Errea *et al.*[37] The similarity shows why the main transitions in the $Be^{4+}+H_2$ reaction occur[5] between the two states described in the previous paragraph: all other avoided crossings in Figs. 3 appear as *real* crossings in Fig. 4 (because of the increased symmetry[38] for the single-electron diatomic); accordingly, when the H atom is replaced by a H_2 molecule, the crossings become extremely sharp avoided crossings.

The relation between the diagrams of Figs. 3 (or Figs. 4) and Fig. 5 can be further analysed. First, in both diagrams the pseudocrossings occur because of the different asymptotic behavior of entrance and exit channel energies. In particular, the Be^{3+} ion interacting with the charged H_2^{+} molecule in Ψ_{sct}, the orbital χ_{Be} appearing in expression (1) is a hybrid combination of the $3s$, $3p$, and $3d$ orbitals of Be^{3+}.

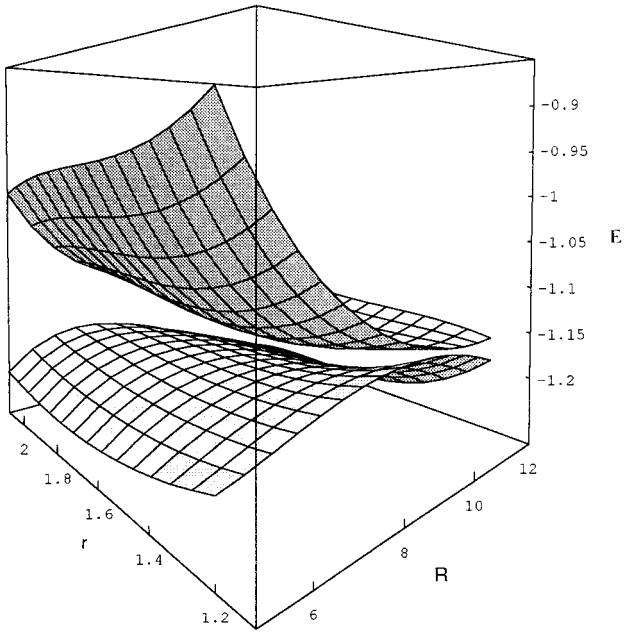

FIG. 8. Radial dependence of the PES's of the entrance and main exit channel considered in this work. Plot of the electronic energies (in hartree), as functions of the Be–H (R) and H–H (r) distances (in bohr), for a collinear geometry ($\theta=0°$).

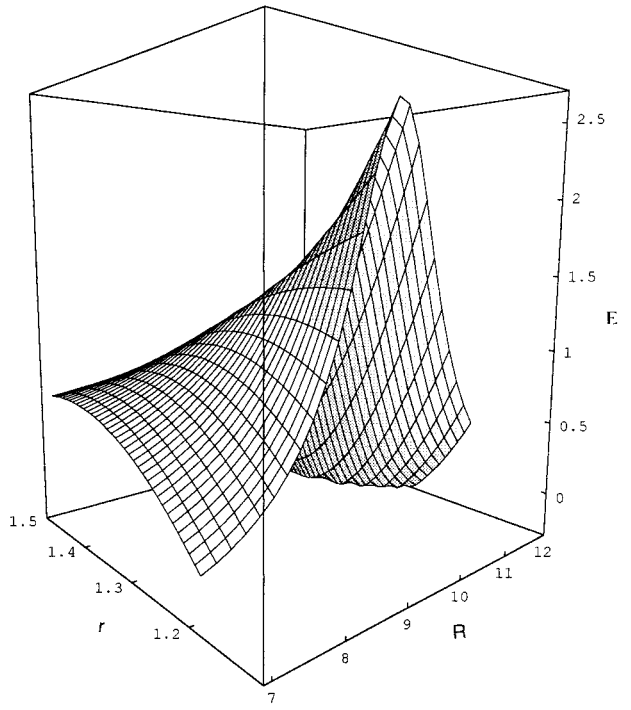

FIG. 9. Radial dependence of the nonadiabatic coupling M [Eq. (2)], between the entrance and main exit channel considered in this work. Plot of M (in $bohr^{-1}$), as a function of the Be–H (R) and H–H (r) distances (in bohr), for a collinear geometry ($\theta=0°$).

The same holds in the diatomic case, where the hybridization of the Be^{3+} ion is due to the proton. The Be^{3+} hybrid has a dipole moment which interacts with the charge of the ionic partner (H_2^+ or H^+), yielding a R^{-2}-varying term. The pseudocrossing position is then given as the R value where the $Be^{3+}+H_2^+(H^+)$ interaction, roughly given by the $3/R$ Coulomb repulsion plus this ion–dipole term, equals the asymptotic energy energy difference with the entrance channel $Be^{4+}+H_2(H)$. The situation is thus the same for the di- and triatomic, and is slightly different from the usual ionic–covalent transitions, where, except for small R^{-4}-varying induction terms, the transition region is only determined by the Coulomb interaction in the ionic state. With respect to the quantitative differences between the diagrams of Figs. 3(b) (for example) and 5, they are easily seen to be a consequence of the fact that the energy difference between entrance and exit channel is 0.389 hartree at infinite R for the diatomic case, and 0.282 hartree for the triatomic, for $\theta=0°$ and $r=1.4$ bohr. As a consequence, the pseudocrossing is displaced to larger values of R in the triatomic. Furthermore, since the exchange interaction between the Be ion and the hydrogen atom or molecule decreases exponentially with R (see Sec. II A), this displacement is accompanied by a narrowing of the energy gap at the corresponding pseudocrossing between the adiabatic energies. These differences are less marked at larger r values [see Figs. 3(c), 4(c)], because the energy difference between H_2 and H_2^+ then decreases, and the molecular energy diagram for the triatomic becomes closer to that for the diatomic.

C. Potential energy and dynamical coupling surfaces

1. Angular dependence

Even with the reduction to a two-state problem, the visualization of the pertinent molecular data (PES's and dynamical coupling), which are functions of the ''bond'' lengths R, r, and the angle θ between them, requires ''cuts'' of these four dimensional surfaces. Fortunately, as we shall now see, the angle θ is easily dispensed with in the discussion. Figure 6 displays the energy surfaces for the entrance and exit channels, and Fig. 7 the nonadiabatic coupling between them as functions of R and θ (in degrees), for $r=1.4$ bohr. As in Fig. 3, the two PES's avoid crossing at a value $R\approx 9$ a.u. that is almost independent of θ; accordingly, the radial coupling exhibits a corresponding Lorentzian ridge. The weak anisotropy of the data is caused by the small angular dependence of the position and width of the pseudocrossing. This is in turn due to the little variation of the entrance channel PES, and the isotropy of the Coulomb and charge–dipole interactions in the exit channel. Nevertheless, because of higher order intermolecular forces, the data are not completely isotropic, and there is an increase of ≈ 0.5 bohr in the pseudocrossing position between the $\theta=0°$ and $\theta=90°$ values. This variation is almost independent of the internuclear distance r of the diatomic.

2. Radial dependence

We present in Figs. 8 and 9 the variation of the PES's and the M coupling with R and r, for $\theta=0°$. It will be no-

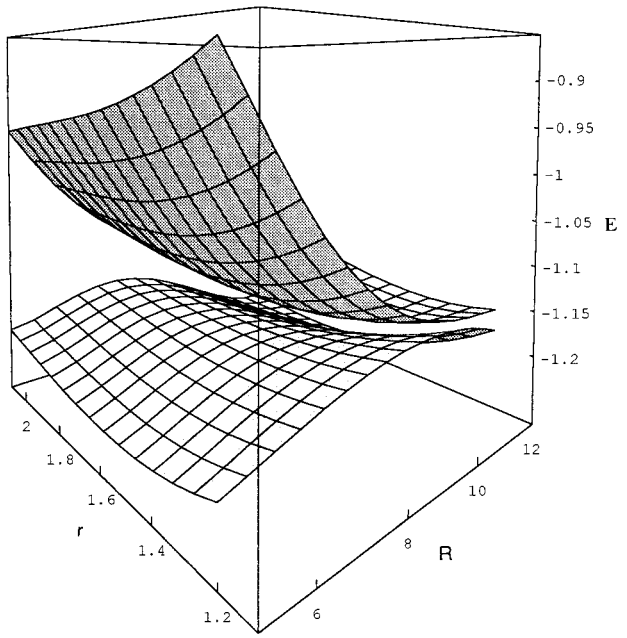

FIG. 10. Radial dependence of the PES's of the entrance and main exit channel considered in this work. Plot of the electronic energies (in hartree), as functions of the Be–H (R) and H–H (r) distances (in bohr), for a perpendicular geometry ($\theta=90°$).

ticed that these data, as well as the ''cuts'' in Figs. 3 and 4, display a marked variation with the value of the internuclear distance r of the diatomic. This holds for all orientations of this molecule; as an illustration, the PES's for $\theta=90°$ are given in Fig. 10. The strong r dependence was found[5] to have a major effect on the dynamics, and in particular on the vibrational state dependence of the capture cross section. In particular, it precludes the use of Franck–Condon-type approximations[17,18,39] up to rather high collision energies $E>9$ keV, because the validity of these approximations hinges on a small variation of the transition amplitudes with the corresponding vibrational coordinate. It is therefore important to understand why we have a steep variation in the present case.

The r dependence of the molecular data can be directly related to the energy values at infinite R. For 1.4 bohr$<r<2$ bohr (approximately), the H_2^+ energy diminishes with r, while that of the H_2 molecule increases. Accordingly, the energy difference between entrance $Be^{4+}+H_2$ and exit $Be^{3+}+H_2^+$ channels significantly increases with r, for fixed R values. Since the pseudocrossing position is roughly given by three times the inverse of the energy difference, we see that this position also diminishes with r. As explained above, the energy gap at the pseudocrossing decreases exponentially with its position, so that when r increases we obtain a wider avoided crossing (Fig. 8) and a flatter coupling (Fig. 9). For 1 bohr$<r<$1.4 bohr, both energies decrease with r, but that of H_2^+ ionization decreases faster, with the same final behavior that at larger r values.

It is customary[10,19] in many applications to employ the

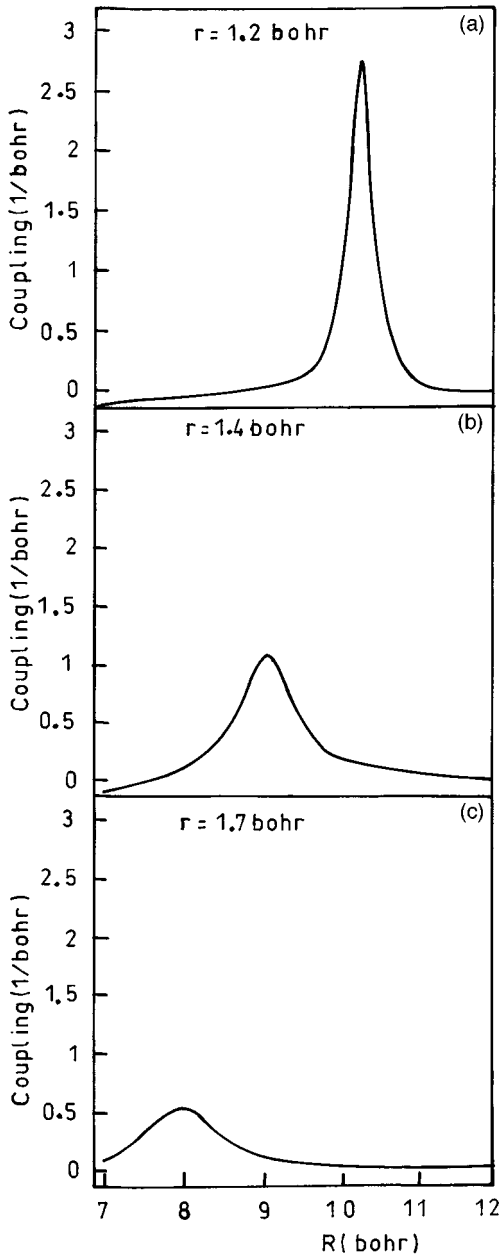

FIG. 11. Strong r dependence of the nonadiabatic couplings. Plot of the nonadiabatic coupling M [Eq. (2)], between the entrance and main exit channel considered in this work, as a function of the Be–H distance R (in bohr), for a collinear geometry ($\theta=0°$), and for the H–H distances: (a) $r=1.2$ bohr; (b) $r=1.4$ bohr; and (c) $r=1.7$ bohr.

Landau–Zener model[35,36] of electronic transitions, which is a Lorentzian fit of the coupling

$$M(R,r,\theta)\approx\frac{\lambda/2}{(R-R_0)^2+\lambda^2}, \tag{9}$$

where $R_0(r,\theta)$ is the pseudocrossing position, and $\lambda(r,\theta)$ a parameter yielding the width of the peak. By a fit of our calculated couplings, made by taking $(2\lambda)^{-1}$ to be the peak value, we have explicitly checked that for $r<1.85$ bohr the model reproduces correctly the transition probabilities, within the usual limitations.[16,36] For $r>1.85$ bohr, expression

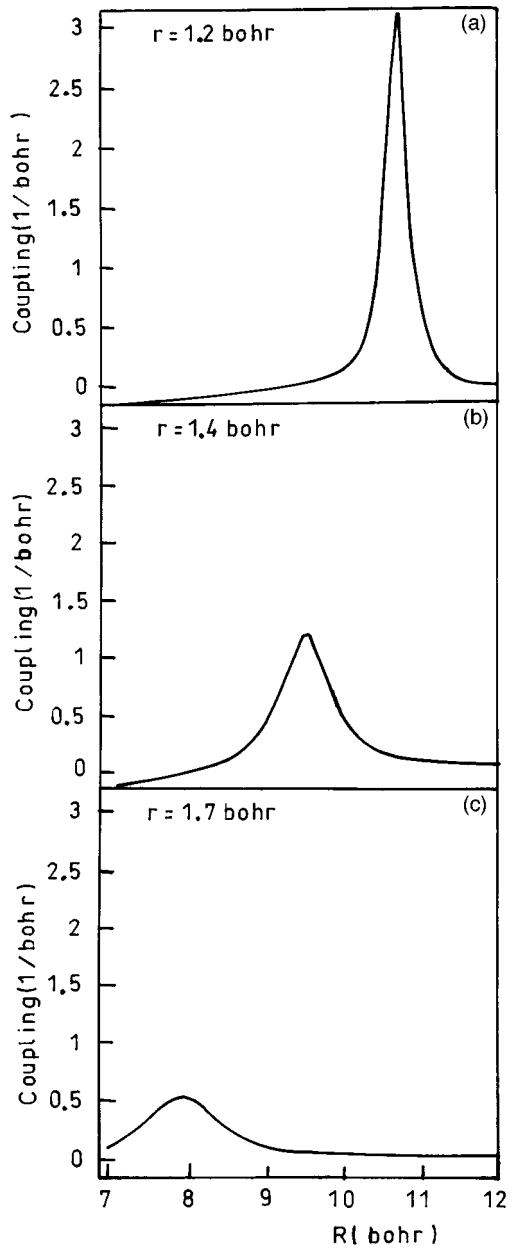

FIG. 12. Same as in Fig. 11, for a perpendicular geometry (θ=90°).

(9) is inaccurate, and the Landau–Zener method can then produce cross sections that are in error by several orders of magnitude.

Incidentally, when Eq. (9) is accurate, use of Eq. (8) yields a corresponding expression for the radial coupling along the vibrational coordinate

$$N(R,r,\theta)\approx M\lambda\,\frac{\partial}{\partial r}\left(\frac{R-R_0}{\lambda}\right). \tag{10}$$

For future applications, it is useful to display in more detail the main features of the molecular data. This requires cuts of the previous surfaces for fixed r values, to be examined together with the 3D plots. These data are given in Figs. 3 (θ=0°) and 4 (θ=90°), for the energies and Figs. 11 (θ=0°) and 12 (θ=90°) for the coupling.

IV. CONCLUSIONS

We have presented the main characteristics of the potential energy and nonadiabatic coupling surfaces for the BeH_2^{4+} quasimolecule, that are relevant to the dynamics of electron capture in $Be^{4+}+H_2$ collisions in the 50 eV amu$^{-1}<E<1$ keV amu^{-1} energy range. While the molecular data and dynamical processes are similar to those of $Be^{4+}+H$ collisions, there appears a striking difference with respect to the use of standard programs of quantum chemistry to calculate the data. This property, which prompted a separate publication of the statical and dynamical treatments, is due to the fact that entrance and exit electronic states are infinitely excited, and therefore a special, block-diagonalization procedure had to be set up. These characteristics are common to all $X^{q+}+H_2$ collisions involving bare ions, among other cases, so that the description of our implementation should be of general usefulness. In addition, the present work reported the first systematic application of our modified[7] MELD program[6] to calculate nonadiabatic couplings.

For the specific case of the BeH_2^{4+} system, we found that for the energy range considered two states are mainly involved, and the corresponding PES and dynamical coupling have been presented in detail. These data display little dependence upon the ''bond'' angle θ, but a strong one on the H–H ''bond'' distance. This has important dynamical consequences,[5] such as the inapplicability of Franck–Condon-type approximations for $E<9$ keV. An open question is the generality of these findings for other $X^{q+}+H_2$ collisions—that is, whether the present system can be considered as a prototype, or is on the contrary an exceptional case. To answer it will obviously require some treatments on other multicharged ion-molecule systems.

ACKNOWLEDGMENTS

This work has been partially supported by the DGICYT Project No. PB93-0288-C02 and was performed in the frame of the agreement No. 8611/CF with the International Atomic Energy Agency. E.S.K. acknowledges Grant No. SAB 94-0271 from the Ministerio de Educación y Ciencia (Madrid).

[1] R. K. Janev and H. Winter, Phys. Rev. **117**, 265 (1985).
[2] H. B. Gilbody, Adv. At. Mol. Phys. **22**, 143 (1986).
[3] L. F. Errea, C. Harel, H. Jouin, L. Méndez, B. Pons, and A. Riera, J. Phys. B **27**, 3603 (1994).
[4] D. E. Dombroswski, E. B. Desknis, and M. A. Pick, in *Atomic and Plasma Interactions Data for Fusion* (International Atomic Agency, Vienna, 1994), Vol. 5, p. 19.
[5] L. F. Errea, J. D. Gorfinkiel, C. Harel, H. Jouin, A. Macías, L. Méndez, B. Pons, and A. Riera, Phys. Scr. **T66**, 33 (1996).
[6] A description of the program can be found in E. R. Davidson, *MOTECC, Modern Techniques in Computational Chemistry*, edited by E. Clementi (ESCOM Science, Leiden, 1990).
[7] J. F. Castillo, L. F. Errea, A. Macías, L. Méndez, and A. Riera, J. Chem. Phys. **103**, 2113 (1995).
[8] D. Searles and E. von Nagy-Felsobuki, *Ab initio Variational Calculations of Molecular Vibrational-Rotational Spectra*, Lecture Notes in Chemistry (Springer, Berlin, 1993).
[9] N. C. Handy, J. F. Gaw, and E. D. Simandiras, J. Chem. Soc. Faraday Trans. 2 **83**, 1577 (1987).
[10] H. Nakamura, *State-Selected and State-to-State Ion–Molecule Reaction*

Dynamics, Part 2, edited by M. Baer and C. Ng, Adv. Chem. Phys. Series **82**, 243 (1992), and references therein.
[11] E. A. Hylleraas and B. Undheim, Z. Phys. **65**, 759 (1930).
[12] J. K. L. McDonald, Phys. Rev. **43**, 830 (1933).
[13] V. López, A. Macías, R. D. Piacentini, A. Riera, and M. Yáñez, J. Phys. B **11**, 2889 (1978).
[14] A. Macías and A. Riera, Phys. Rep. **90**, 299 (1982).
[15] A. Riera, *Time Dependent Quantum Molecular Dynamics*, edited by J. Broeckhove and L. Lathowers (Plenum, New York, 1992).
[16] E. E. Nikitin, *Theory of Elementary Atomic and Molecular Processes in Gases* (Clarendon, Oxford, 1974).
[17] M. S. Child and M. Baer, J. Chem. Phys. **74**, 2832 (1981).
[18] V. Sidis, Adv. At. Mol. Opt. Phys. **26**, 261 (1990).
[19] S. Chapman, *State-Selected and State-to-State Ion–Molecule Reaction Dynamics*, Part 2, edited by M. Baer and C. Ng, Adv. Chem. Phys. Series **82**, 423 (1992), and references therein.
[20] E. A. Gislason, G. Parlant, and M. Sizun, *State-Selected and State-to-State Ion–Molecule Reaction Dynamics*, Part 2, edited by M. Baer and C. Ng, Adv. Chem. Phys. Series **82**, 321 (1992), and references therein.
[21] B. T. Sutcliffe, Mol. Phys. **48**, 561 (1983).
[22] H. S. Taylor, Adv. Chem. Phys. **18**, 91 (1970).
[23] A. Macías, R. Mendizábal, F. Pelayo, A. Riera and M. Yáñez, J. Mol. Struct. (Theochem) **107**, 245 (1984).
[24] A. Macías, R. Mendizábal, F. Pelayo, A. Riera, and M. Yáñez, Phys. Rev. A **33**, 242 (1986).
[25] H. Feshbach, Ann. Phys. **5**, 357 (1958).
[26] H. Feshbach, Ann. Phys. **19**, 287 (1962).
[27] F. Martín, A. Riera, and M. Yáñez, J. Chem. Phys. **84**, 5412 (1986).
[28] F. Martín, A. Riera, and M. Yáñez, Phys. Rev. A **34**, 4675 (1986).
[29] F. Martín, A. Riera, and M. Yáñez, J. Chem. Phys. **86**, 6927 (1987).
[30] I. Cooper, J. Phys. B **24**, 1517 (1991).
[31] L. F. Errea, B. Herrero, L. Méndez, O. Mó, and A. Riera, J. Phys. B **24**, 4049 (1991).
[32] R. Khrishnan, J. S. Binkley, J. S. Seeger, and J. A. Pople, J. Chem. Phys. **72**, 650 (1980).
[33] J. C. Slater, *Quantum Theory of Molecules and Solids* (McGraw-Hill, New York, 1963), Vol. 1, p. 18.
[34] L. Wolniewicz and K. Dreizler, J. Chem. Phys. **88**, 3861 (1988).
[35] E. E. Nikitin, Adv. Quantum Chem. **5**, 185 (1970).
[36] M. S. Child, *Molecular Collision Theory* (Academic, London, 1974).
[37] L. F. Errea, J. D. Gorfinkiel, C. Harel, H. Jouin, A. Macías, L. Méndez, B. Pons, and A. Riera, Phys. Scr. **T62**, 27 (1996).
[38] J. D. Power, Philos. Trans. R. Soc. **274**, 663 (1973).
[39] D. Dhuic, J. C. Brenot, and V. Sidis, J. Phys. B **18**, 1395 (1985).